J Appl Electrochem (2007) 37:1475–1484
DOI 10.1007/s10800-007-9375-4

ORIGINAL PAPER

Carbon supported Ru–Se as methanol tolerant catalysts for DMFC cathodes. Part I: preparation and characterization of catalysts

**G. Zehl · P. Bogdanoff · I. Dorbandt · S. Fiechter ·
K. Wippermann · C. Hartnig**

Received: 1 December 2006 / Revised: 11 July 2007 / Accepted: 13 July 2007 / Published online: 2 August 2007

Abstract Carbon supported $Ru_xSe_yO_z$ catalysts were prepared from $Ru_3(CO)_{12}$ and $RuCl_3 \cdot xH_2O$ as ruthenium precursors and H_2SeO_3 and $SeCl_4$ as the selenium sources. Highly active catalysts for the oxygen reduction reaction (ORR) in direct methanol fuel cells (DMFC) were obtained via a multi-step preparation procedure consisting of a CO_2-activation of the carbon support prior to the preparation of a highly disperse Ru particles catalyst powder that is subsequently modified by Se. Ultimately, an excess of Se was removed during a final thermal annealing step at 800 °C under forming gas atmosphere. The morphology of the catalysts was analyzed by transmission electron microscopy (TEM) and X-ray diffraction (XRD), which shows that the catalysts consist of crystalline Ru-particles with sizes ranging from 2 to 4 nm exhibiting a good dispersion over the carbonaceous support. The corresponding catalytic activity in the process of oxygen reduction was analyzed by cyclic voltammetry (CV) and rotating disk electrode (RDE) measurements. The nature of the carbon support used for the preparation of RuSe cathode catalysts is of significant importance for the activity of the final materials. Catalysts supported on CO_2-activated Black Pearls 2000 gave the highest ORR-activity. Se stabilizes the Ru-particles against bulk oxidation and actively contributes to the catalytic activity. An exceptional property of the carbon supported Ru-particles modified with Se is their resistance to coalescence up to temperatures of 800 °C under inert or reducing conditions. Additional effects of Se-modification are the enhanced stability towards electrochemical oxidation of Ru and a lowering of the H_2O_2 formation in the ORR.

Keywords Ruthenium–selenium cathode catalyst · Oxygen–reduction reaction · Methanol-tolerance · Direct methanol fuel cells

1 Introduction

Commercial DMFC technology is today almost exclusively bound to the use of rare and expensive Pt. By mid 2006 it reached a record value of 1,336 USD/oz. [1] and autocatalysts will continue to drive the market as emission standards are tightened and enforced [2]. Beside this, the use of Pt-based electrocatalysts for DMFC cathodes is hampered by the high mobility of Pt-particles on carbonaceous supports, leading to aggregation and loss of active surface [3]. Even more important, the sensitivity of Pt towards the presence of methanol in the cathode compartments of a cell stack entails catalyst depolarization [4]. Several approaches are described to overcome these disadvantages: (1) The use of Pt-based alloys is considered. However, such catalysts are still expensive and residual methanol sensitivity remains [5]. (2) Inexpensive and methanol tolerant Fe–Co–C catalysts have been suggested [6, 7], but the development status of these systems is far from commercial application. (3) Ru-catalysts modified with selenium ($RuSe_x$) feature excellent methanol tolerance [8]. Nevertheless for the purpose of a successful

G. Zehl (✉) · P. Bogdanoff · I. Dorbandt · S. Fiechter
Hahn-Meitner-Institute-Berlin, Glienicker Str. 100, 14109
Berlin, Germany
e-mail: gerald.zehl@hmi.de

K. Wippermann
Research Center Jülich, IEF-3, 52425 Jülich, Germany

C. Hartnig
Center for Solar Energy and Hydrogen Research
Baden-Württemberg, Helmholtzstraße 8, 89081 Ulm, Germany

commercialization of Ru-based DMFCs, a further improvement of the mass specific activity of these catalysts is desirable. Preceding papers demonstrated the potential to further increase the oxygen reduction activity of $RuSe_x$-based electrocatalysts, while maintaining their superior methanol tolerance [9]. Although the abundance of Ru is comparable to Pt, its price presently amounts to only 42% of that of Pt. The annual mining output sums up to ~120 kg Ru compared to 30 t for Pt. This fact throws light on the restricted industrial demand of Ru at present. Today Ru is primarily obtained as a byproduct of Pt refining. Therefore, with increasing demand the mining of specific Ru-rich ore deposits should not necessarily lead to higher prices for Ru.

$RuSe_x$-catalysts for the oxygen reduction reaction (ORR) were disclosed in 1989 by Chatzitheodorou [10] and the preparation of these systems via thermolysis has been improved [11–13]. Structural characterizations of the active material revealed the existence of a Ru-core decorated with a Se-containing shell of complex structure [14]. It was shown that the presence of Se is the decisive factor to significantly improve the catalytic activity and stability compared to unmodified Ru-nanoparticles. The high activity of the catalyst is due to a special selenization in the course of a one-step preparation technique [15]. However, for commercial application in DMFCs the catalyst activity was still not satisfactory. Undesired catalyst particle aggregation and a shell of amorphous Se-containing byproducts were identified as limiting factors. Although a subsequent thermal annealing step gave higher activities due to reduced thickness of the amorphous particle shell, persistent particle aggregation kept the batch-to-batch reproducibility poor.

A significant leap forward has been achieved by introducing a two-step preparation process. As showed by Hilgendorff et al., the formation of Ru-nanoparticles and the subsequent modification with Se can be optimized separately [12, 13]. According to the Bönnemann synthesis route [16], highly dispersed Ru on a carbon black support was obtained by reduction of Ru-salts in solution followed by depositing the colloidal Ru-particles onto carbon black (e.g., Vulcan XC-72). In a subsequent preparation step, the surface of these Ru-particles was then modified with Se. Elemental Se was deposited in a common impregnation/adsorption process followed by partial oxidation in air and subsequent reduction under hydrogen atmosphere. The resultant $RuSe_x$ catalysts showed a significantly higher activity due to the improved dispersion of the catalytically active particles [12, 13]. Furthermore, all these preparation techniques lead to a product where Se is firmly bound to Ru exhibiting a thermal stability up to 850 °C under inert conditions [14, 17]. Hence, no release of poisonous Se or Se-compounds is expected in electrochemical experiments under reducing conditions. However, this preparation procedure was rather complex and the Se-loading was still unsatisfactory with respect to the extent of surface modification and its reproducibility. Therefore, the objective of this work is to optimize the catalyst preparation towards reproducible and simplified preparation routes and higher catalytic activities in the ORR as well as to provide adequate amounts of high-performance catalysts for the preparation of catalyst coated membranes (CCM) and their characterization in membrane electrode assemblies (MEA). These results will be discussed in Part II of this contribution [18].

2 Experimental

2.1 Preparation of electrocatalysts

2.1.1 *Ru(20 wt.%)/Vulcan-intermediates from $Ru_3(CO)_{12}$-thermolysis modified with H_2SeO_3*

$RuSe_x$/C-catalysts with a Ru-loading of 20 wt.% were obtained by preparing Ru(20 wt.%)/C-intermediates and their subsequent selenization with H_2SeO_3. Ru/C-intermediates were prepared via the carbonyl route adapted from Hilgendorff et al. and described in [12]. In brief, an amount of 1.3 g $Ru_3(CO)_{12}$ was dissolved in 250 ml of toluene under reflux at ~110 °C for 15 min under argon atmosphere. Then, this solution was slowly added to a suspension of 0.8 g carbon (Vulcan XC-72) in 250 ml of toluene at room temperature under air. The solvent was subsequently rotary evaporated at 40 °C. The obtained $Ru_3(CO)_{12}$ coated carbon powder was finally reductively annealed at 300 °C under hydrogen for 2 h. For their selenization, an amount of 0.5 g of the Ru/C-powders was dispersed in 200 ml H_2O containing 1.54 g (0.06 mol/l), 0.154 g (6 mmol/l), 15.4 mg (0.6 mmol/l) and 1.5 mg (0.06 mmol/l) H_2SeO_3, respectively (see Table 1). The powders were afterwards filtered and dried in air without further flushing. Finally, a reductive treatment under forming gas (5%H_2/95%N_2) for 30 min at 300 °C was performed.

2.1.2 *Ru(20 wt.%)/Vulcan and Ru(40 wt.%)/Vulcan ETEK catalysts modified with H_2SeO_3*

The commercially available Ru/C-catalysts from ETEK with nominal Ru-loadings of 20 and 40 wt.% supported on Vulcan XC-72 were used as starting materials. At first, the ETEK materials were reductively annealed at 250 °C under flowing hydrogen for 20 min in a horizontal quartz tube split hinge furnace. For the selenization of the reduced

Table 1 Effect of H_2SeO_3 treatment on the Se-content and the catalytic activity of $RuSe_x$/C-catalysts, adopted from [19]

H_2SeO_3 concentration (mol l^{-1})	Selenium content in the catalyst from NAA (%)	ORR activity at 0.7 V (NHE) from RDE data (mA cm^{-2})
0	0	0.5
6×10^{-5}	0.14	1.6
6×10^{-4}	0.63	2.4
6×10^{-3}	1.23	3.1
6×10^{-2}	4.52	2.2

The Ru-content in the catalysts was 20 wt.%. The Ru-concentration on the RDE was 70 μg_{Ru} cm^{-2}

Ru(20 wt.%)/Vulcan and Ru(40 wt.%)/Vulcan ETEK-samples, an amount of 0.5 g was dispersed in 200 ml H_2O containing 154 mg (6 mmol/l) and 308 mg (12 mmol/l) H_2SeO_3, respectively. Afterwards, the powders were filtered and dried in air without further flushing. Finally, a reductive treatment under forming gas (5%H_2/95%N_2) for 30 min at different temperatures ranging from 150 to 900 °C was performed.

2.1.3 *Ru(20 wt.%)/C and Ru(40 wt.%)/C catalysts supported on CO_2 activated carbon blacks and modified with $SeCl_4$*

For the catalyst preparation via the ruthenium chloride route a calculated amount of $RuCl_3 \cdot xH_2O$ (metal content 35 wt.%) was dissolved in water, previously purged with argon. This precursor solution was placed in a round-bottomed flask at the end of a horizontally aligned quartz tube which was inserted into a split hinge furnace. The carbon support had to be activated prior to the impregnation with the active metals. Therefore, the carbon support sample (Black Pearls 2000® from Cabot) was placed inside the tube, purged with CO_2, heated from room temperature to 950 °C with a heating rate of 7.5 K min^{-1} and held at this temperature for 20 min. The samples were then allowed to cool under flowing CO_2. The gas flow rate during all steps was held constant at 7.5 l min^{-1}. Afterwards, the activated carbon sample was transferred into the round-bottomed flask connected to the end of the quartz tube furnace. This geometry was used to avoid any changes of the surface chemistry of the activated carbons by air contact during the transfer of the treated materials into the solution. The resultant suspensions were agitated ultrasonically. Afterwards, the solvent was removed by rotary evaporation and the dried catalyst powder was treated under forming gas (5%H_2/95%N_2) at a temperature of 200 °C. The resultant material was rinsed with water to remove all chlorine containing residues. Finally, it was dried in a desiccator.

To selenize the Ru/C-intermediate, $SeCl_4$ was dissolved in dried and deaerated acetone. This solution was placed in a round-bottomed flask connected directly to the exit of the tube furnace, whereas the Ru/C-material was placed into the tube furnace. After treating the Ru/C-powder with forming gas (5%H_2/95%N_2) at 200 °C to clean up the surface from any impurities, it was transferred into the acetonic solution of $SeCl_4$ excluding air contact. After ultrasonic conditioning the acetone solvent was removed by rotary evaporation. Finally, a reductive treatment under forming gas for 30 min at different temperatures was performed.

2.2 Electrochemical characterization

The catalytic activity of the samples was determined via cyclic voltammetry (CV) and rotating disk electrode (RDE) measurements. The preparation of the electrodes was described elsewhere [9, 12, 13, 15]. In brief, for both techniques the same conventional one-compartment electrochemical glass cell was used. A mercury sulfate electrode served as reference and a platinum wire as counter electrode. The catalyst powder was attached onto a working electrode, which consists of a PTFE surrounded glassy carbon (GC) rod with a diameter of 3 mm. One mg (1 mg) of the catalyst sample to be characterized was ultrasonically suspended in 200 µl of a 0.2% Nafion® solution (Aldrich, St. Louis, MO, USA). A precise amount of 5 µl of this suspension was then transferred onto the GC electrode and dried in air at 60 °C. The CV and the RDE measurements were performed at room temperature in 0.5 M H_2SO_4, saturated with N_2 and with O_2 respectively.

2.3 X-ray diffractometry (XRD), transmission electron microscopy (TEM) and neutron activation analysis (NAA)

X-ray diffraction (XRD) patterns were recorded from powder samples using a SIEMENS diffractometer D500/D5000 (Cu $K\alpha_1$ radiation, $\lambda = 0.154178$ nm) in Θ–2Θ coupling at a scanning rate of 0.02° s^{-1} for 2Θ ranging from 20 to 60°.

Transition electron microscopy (TEM) images were taken using a Philips CM 12 equipped with a super twin lens with a slow scan CCD camera and an X-ray fluorescence analyzer (EDX). The acceleration voltage was set to 120 kV. The samples were prepared by dispersing a small amount of catalyst in ethanol using an ultrasonic bath. One drop of this suspension was then deposited onto a carbon-coated grid and left to dry at room temperature.

Neutron activation analysis was performed to confirm the concentration of the active metals Ru and Se.

2.4 Thermogravimetry coupled with mass spectrometry (TG-MS)

The thermal evolution of the catalysts was monitored by using a NETZSCH STA409C thermogravimetric analyser (TGA), coupled with a Balzers Quadstar QMG 422 quadrupole mass spectrometer via a skimmer coupling system (TGA-MS). Measurements were carried out under Ar or N_2/H_2 atmosphere. The heating rate was 5 K min^{-1} and the gas flow was 150 ml min^{-1}.

3 Results

3.1 Ru(20 wt.%)/Vulcan-intermediates from $Ru_3(CO)_{12}$-thermolysis modified with H_2SeO_3

Selenization of carbon supported Ru-nanoparticles is considered as the crucial preparation step towards an enhanced ORR-activity of the final catalyst. Therefore, the amount of Se involved in this step should be of major significance for the achievement of an optimum extent of this surface modification. Consequently, a method for a precise adjustment of the Se loading of the catalysts is in demand. Hilgendorff et al. [12, 13] described a promising selenization procedure, affording catalysts with superior RDE activity. However, when employing the Hilgendorff's preparation method, poor reproducibility with respect to the catalyst composition was encountered. The initially suggested multi-step procedure of introducing elemental Se, its partial oxidation and subsequent reduction involves the formation of different volatile Se_x gas species ($2 \leq x \leq 8$) that might be evolved during the reduction step. Congruously, as confirmed by elemental analysis via NAA, the poor reproducibility was due to ill-defined process conditions concerning the amount of Se introduced as well as the part of Se evolving from the catalyst surface during the heat treatment. Therefore, a fundamental improvement of the selenization process was required.

To tweak this preparation step towards better reproducibility, highly dispersed Ru(20 wt.%)/C-intermediates have been prepared as suggested by Hilgendorff, but treating them with selenious acid (H_2SeO_3) afterwards instead of the treatment with dissolved elemental Se. To control the amount of Se adsorbed onto the Ru-particles, aqueous solutions of different H_2SeO_3 concentrations were applied to modify four samples of the same Ru(20 wt.%)/C-powder as described in Sect. 2.1.1. Table 1 summarizes the kinetic current densities of the resulting $RuSe_x$/C-catalysts in the ORR, inferred from RDE measurements, as a function of the concentration of selenious acid employed in the adsorption step [19]. Additionally, the real Se content in the catalyst was verified by NAA.

It was demonstrated that the concentration of Se in the catalyst did not increase linearly with increasing molarity of the H_2SeO_3-solution used in the adsorption step. Apparently, the adsorption of H_2SeO_3 and therefore the amount of Se possible to deposit on the surface of the catalysts are controlled by specific adsorption equilibriums. According to Table 1, the current density increases until a Se-loading of about 1 wt.% is obtained, remaining constant at higher Se-content. It has to be concluded that an optimized Se-concentration on the Ru-surface exists, creating a chemical structure favorable for catalysis of the ORR. Above a certain Se-concentration, catalytically inactive species are formed on the surface of the Ru-particles leading to diminished activity. Taking into account the existence of a certain degree of coverage by Se being optimal from the viewpoint of catalytic activity, higher concentrations of selenious acid should lead to an overload of the Ru-particle surfaces with Se and may cause partial formation of $RuSe_2$.

This assumption was confirmed by thermogravimetric analysis coupled with mass spectrometry (TGA-MS), revealing that elemental Se as well as Se firmly bonded to Ru is present within the catalysts. During the thermal analysis elemental Se was released as volatile species at temperatures around 600 °C, whereas Se associated with the Ru particles could only be removed above 900 °C [14]. However, only Se firmly bonded to the Ru particles exerts a promoting effect on the catalytic reaction (G. Zehl et al. 2006, submitted data).

At the current stage of investigation it is not possible to draw a final conclusion as to how the Se is distributed over the surface of an active Ru-particle to afford maximum catalytic activity. However, the assumption of a preferable extent of a coverage with Se on the Ru-particles implies the existence of an optimum Ru:Se ratio, being analytically accessible more easily. Important parameters to define the optimum Ru:Se ratio are size and surface structure of the Ru-particles. Further, on carbon supported $RuSe_x$-catalysts it should be taken into account that Se is also deposited on the carbon support between the Ru-particles when adsorbed from selenious acid. To our knowledge the distribution between catalytically irrelevant Se on the support and activity promoting Se on the Ru-particles is greatly influenced by the temperature of the thermal treatment applied during the Se-modification [17]. Therefore, as will be shown in the following, alternative preparation routes towards $RuSe_x$-catalysts evoke different optimized Ru:Se ratios, dependant on the respective structural characteristics of the samples.

3.2 Ru(20 wt.%)/Vulcan and Ru(40 wt.%)/Vulcan ETEK catalysts modified with H_2SeO_3

A promising route to nano-disperse $RuSe_x$-particles via the preparation of colloidal metal particles suspensions was described by Bönnemann et al. [16]. However, considering the final goal of catalyst mass production in a streamlined preparation process, it would be desirable to provide these products by a less laborious and expensive procedure. Meanwhile, finely dispersed Ru on carbon black with narrow particle size distribution is a commercially available state of the art product. The subjection of such a commercial Ru/C intermediate to a subsequent selenization step as described above may represent a simplified preparation route towards higher active $RuSe_x$-catalysts, allowing studying the influence of the Se-promoter avoiding fluctuations in the constitution of the Ru-particles. Following this idea, commercial Ru/C catalysts from ETEK (20 and 40 wt.% Ru deposited on Vulcan XC-72) were treated with H_2SeO_3. An adequate Se-content of the final catalyst was achieved by adjusting the concentration of the aqueous H_2SeO_3-solution according to the best results from Table 1. In detail, a Ru(20 wt.%)/Vulcan and a 40 wt.% Ru/Vulcan ETEK-catalyst were treated with a 6×10^{-3} M or a 1.2×10^{-2} M solution of H_2SeO_3 as described in Sect. 2.1.2. to yield a Se-content of 1.5 and 2.8 wt.%, respectively. The final preparation step encounters the formation of a surface structure, chemically favorable for the ORR. Based on the so far established preparation techniques, annealing in H_2 atmosphere was employed as before. Due to the expected impact of the annealing temperature as revealed from TG-MS, temperatures ranging from 100 to 900 °C were applied for different samples to study this temperature influence.

Figure 1 shows kinetic current densities at 0.7 V NHE from RDE measurements of the catalysts annealed in forming gas atmosphere versus the annealing temperature. An optimum was reached at a temperature in the range 200–500 °C. Above that range, a decrease in current density is observed. However, TG-MS measurements and electrochemical analyses revealed that the firmly bound Se responsible for the promoting influence on the ORR activity is only released at temperatures above 800 °C. Hence, the decline in activity observed already at temperatures between 500 and 800 °C can not be explained by the loss of the Se-promoter alone. Additionally, at temperatures above 500 °C a pronounced particle growth is initiated leading to a reduced active surface. This could be verified by XRD and TEM measurements (see Figs. 2, 3). After annealing at 500 °C, coalescence of particles is observed combined with the formation of facetted particles with sizes larger than 10 nm after annealing at $T > 700$ °C. These findings are confirmed by a continuous decrease in the full width half maxima (FWHM) of the Ru powder diffraction lines.

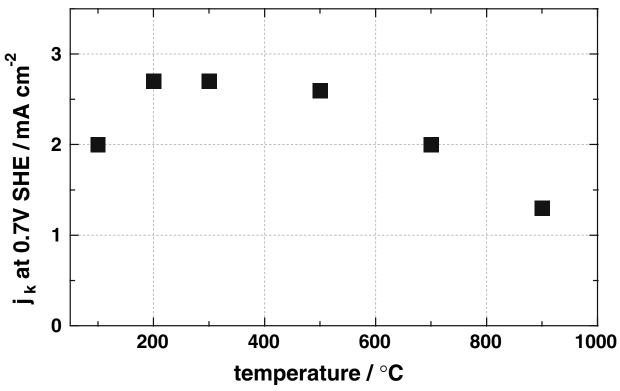

Fig. 1 Influence of the thermal annealing temperature on the catalytic activity of a Ru(20 wt.%)/Vulcan ETEK-catalyst modified with H_2SeO_3, as inferred from RDE-measurements in 0.5 M H_2SO_4

When modifying commercial Ru(20 wt.%)/Vulcan and Ru(40 wt.%)/Vulcan ETEK-catalysts with Se by adsorption of H_2SeO_3 and subsequent reductive annealing at 300 °C, concentrations of 1.5 and 2.8 wt.% Se, respectively, were found to be preferable. To illustrate the achievements with respect to the ORR-activity attained so far, the I/U-curve of the most active Ru(40 wt.%)Se(2.8 wt.%)/Vulcan catalyst is given in Fig. 4, compared with the I/U-curves of the unmodified Ru(40 wt.%)/Vulcan ETEK-catalyst and of a commercial Pt(40 wt.%)/Vulcan reference catalyst from Heraeus. Figure 4 shows the highly improved ORR-activity of the $RuSe_x$/C catalysts in RDE measurements, although there still remains an activity gap to the Pt/C reference catalyst. Se modified Ru-catalysts were further tested in DMFC cathodes at the Research Center Jülich. The results of this investigation are described separately in part II of this contribution [18].

3.3 Ru(20 wt.%)/C and Ru(40 wt.%)/C catalysts supported on CO_2 activated carbon blacks and modified with $SeCl_4$

The Se-modification of a commercial Ru/C catalyst represents an easy and convenient approach to obtain Ru-based catalysts with enhanced ORR-activities. However, structural investigation suggests potential for further improvements. At first, the commercial Ru/C catalysts feature relatively large Ru-particle sizes of 2.4 and 5 nm for 20 and 40 wt.% metal content, respectively. Therefore, a larger active surface can be made available, when higher Ru-loadings are accompanied with an enhanced fraction of smaller particles. Furthermore, higher annealing temperatures have been found to be advantageous to remove excess

Fig. 2 TEM-images of the final Ru(20 wt.%)Se/Vulcan catalysts obtained after reductive annealing at different temperatures: (**a**) 200 °C, (**b**) 300 °C, (**c**) 500 °C and (**d**) 700 °C, respectively. For catalyst performances of these samples see Fig. 1

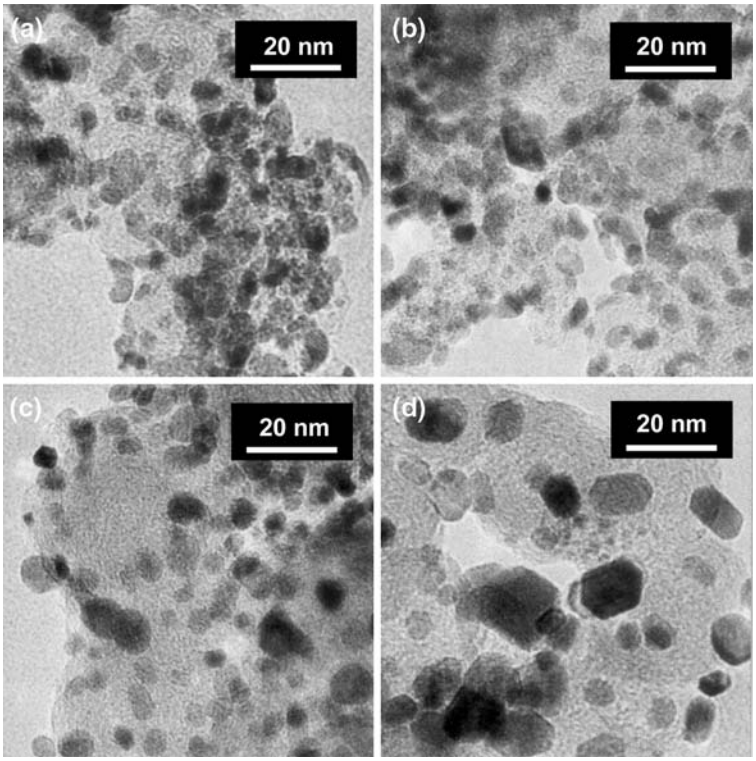

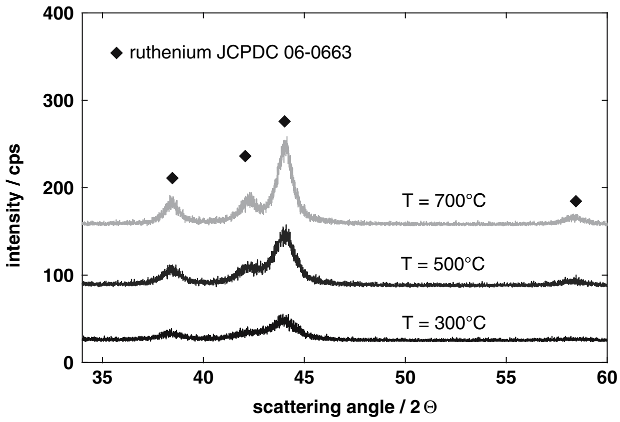

Fig. 3 XRD pattern of the final Ru(20 wt.%)Se/Vulcan catalysts obtained after hydrogen treatment at different temperatures, for additional information see Fig. 2

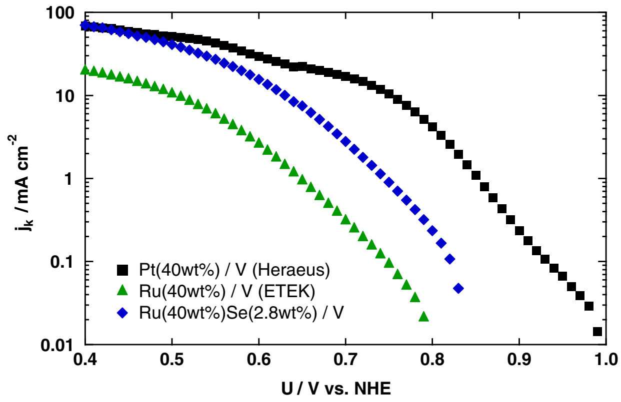

Fig. 4 Tafel plots for the oxygen reduction over various Ru-based catalysts compared with a Pt(40 wt.%)/Vulcan (Heraeus) reference catalyst, as obtained from RDE-measurements in 0.5 M H_2SO_4

Se introduced during the selenization step. A restriction of the undesired particle growth at such temperatures should reduce activity losses. Both disadvantages of the commercial Ru/C catalysts, larger particles at higher loading and extended particle growth at higher temperatures, encouraged searching for new synthesis routes. Novel preparation techniques were investigated, affording smaller metal particles even at high Ru-loadings. Preliminary work in our laboratory revealed that the impregnation of carbon blacks with $RuCl_3$ followed by its reduction under forming gas is promising.

Moreover, systematic investigation of commercial carbon supports demonstrated that their activation under CO_2 prior to the first impregnation step has a positive influence on the dispersion of the formed Ru-particles. Thus, especially promising catalysts could be prepared with CO_2-activated Black Pearls 2000® (BP), showing a high and reproducible dispersion of the $RuSe_x$-particles ranging from 1 to 2 nm in size, as confirmed by TEM images (G. Zehl et al. 2006, submitted data). XPS analysis in the O1s region revealed that an enrichment of oxygen containing surface groups takes place during the CO_2 activation [17].

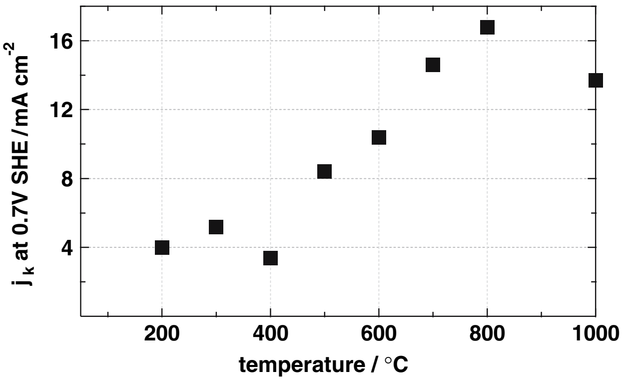

Fig. 5 Current densities from RDE-measurements in 0.5 M H_2SO_4 for the Ru(20 wt.%)Se/BP_{act}-catalyst as function of the temperature of the reductive annealing step after the impregnation of the Ru/BP_{act}-intermediate with $SeCl_4$; support: CO_2 activated Black Pearls 2000; Ru-precursor: $RuCl_3$

Most likely these groups are able to stabilize the polar $RuCl_3$-precursor on the carbon surface during the impregnation process. This, in turn, causes a reduced mobility of Ru on the surface during the subsequent reduction step and facilitates the formation of smaller crystallites. Afterwards, the resulting Ru/BP_{act}-intermediates have to be modified with Se. However, the enlarged surface area of the CO_2-activated support also provides more adsorption sites for the Se-precursor. Consequently, a competitive adsorption of Se on the Ru-particles and on the carbon surface has to be assumed. Therefore, to ensure a proper interaction of Se with the Ru-surface, the Se-precursor should be introduced in excess. Since the adsorption of selenious acid does not allow adequately high Se-loadings to be obtained (due to the limited amount of free adsorption sites), an impregnation technique with deaerated acetonic solution of selenium chloride ($SeCl_4$) was chosen to force larger amounts of Se onto the Ru/C-intermediate, as described in Sect. 2.1.3.

After the formation of the desired $Ru_xSe_yO_z$ structure on the surface of the Ru-crystallites the inactive and furthermore useless excess Se must be removed. As described above, this could be easily achieved at elevated temperatures, where volatile Se-species exist. However, at these severe conditions progressive growth of the modified Ru-particles is expected, accompanied by an undesired loss in catalytic activity. Therefore, in the preceding systematic investigation the Se-loading and the thermal annealing temperature were optimized towards a maximum in RDE-current. Figure 5 shows the kinetic current densities of $RuSe_x$/BP_{act} catalysts obtained at different temperatures of the reductive annealing step after the impregnation of the Ru/BP_{act}-intermediate with $SeCl_4$. It is remarkable that the kinetic current density rises up to 800 °C and decreases only above that temperature, in contrast to the $RuSe_x$/Vulcan-catalyst obtained via adsorption of H_2SeO_3 (see Fig. 1) where current density already decreased above 500 °C. This clear difference in the temperature dependence is also reflected in a significant distinction in the

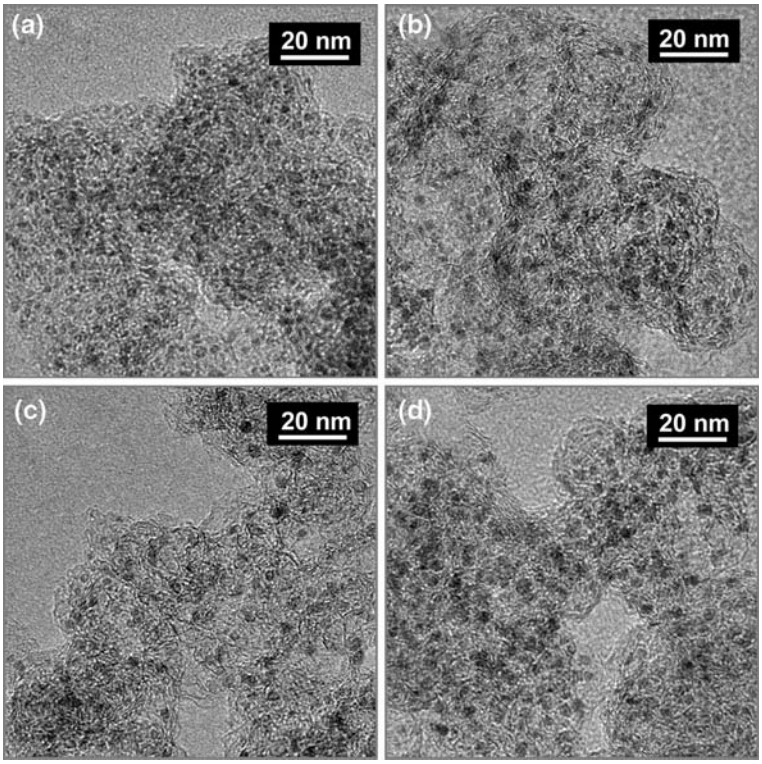

Fig. 6 TEM-images of the final Ru(20 wt.%)Se/C catalysts after reductive annealing at different temperatures: (**a**) 300 °C, (**b**) 500 °C, (**c**) 800 °C and (**d**) 1,000 °C, respectively. The catalyst support was CO_2-activated Black Pearls 2000. The Se-content decreased with rising annealing temperature. For catalyst performances see Fig. 5

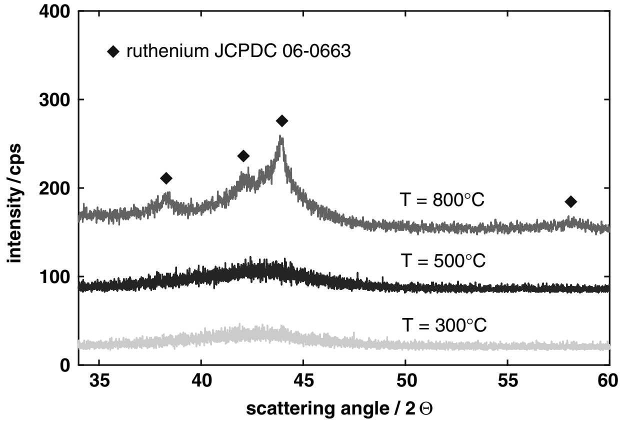

Fig. 7 XRD pattern for a Se-modified Ru(20 wt.%)Se/C catalyst after reductive annealing at different temperatures, for additional information see Fig. 6

extent of particle growth found by TEM and XRD measurements on both catalysts (see Figs. 2–3, 6–7, respectively). No significant particle growth was noticed on the RuSe$_x$/BP$_{act}$ samples at temperatures up to 800 °C (see TEM in Fig. 6 and XRD in Fig. 7), corresponding to the high ORR-activity of samples annealed up to this temperature (see Fig. 8). Moreover, the decrease in activity for annealing temperatures above 800 °C is corroborated by XRD measurements, where decomposition of the RuSe$_x$-nanoparticles was observed, accompanied by the formation of larger metallic Ru-crystallites (see Fig. 7).

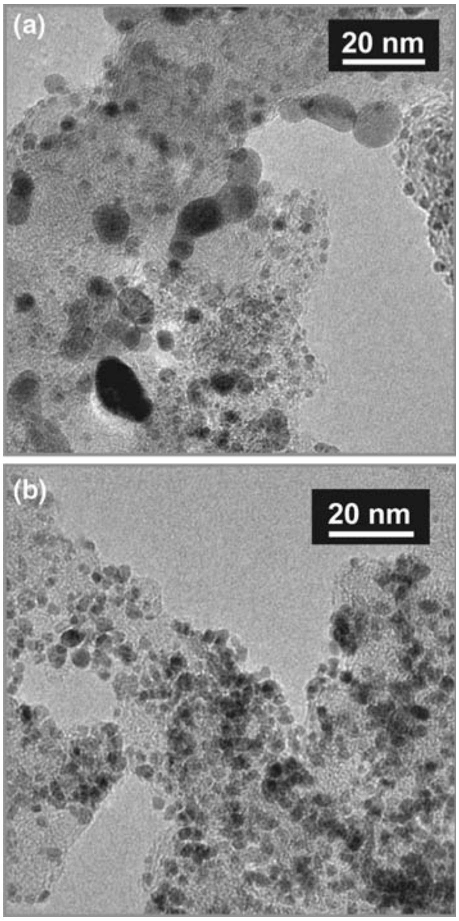

Fig. 8 TEM-images of Ru(40 wt.%)/Vulcan: (**a**) catalyst prepared by impregnation of Vulcan XC-72 without pre-treatment under CO_2, (**b**) catalyst with the same metal loading prepared by impregnation of CO_2-activated Vulcan XC-72. The Ru-precursor was $RuCl_3$

In order to clarify, to what extent the observed stabilization of the Ru-particles is due to the surface properties of the support, Ru-particles deposited on CO_2-activated Vulcan (Ru/V$_{act}$) and on not CO_2-activated Vulcan (Ru/V) were annealed and characterized by TEM. The Ru-content of both catalysts was 40 wt.%. The images presented in Fig. 8 clearly show that CO_2-activation of the support affords smaller Ru-particles. However, the Se-modification was found to be also a crucial factor for the stabilization of the Ru-nanoparticles. After reductive annealing at 800 °C a RuSe$_x$/V-catalyst revealed smaller particle sizes compared to the Ru/V-intermediate treated under the same conditions. Consequently, both, the extent of selenization and the characteristic of the surface of carbon support play an important role. Therefore, we suggest a synergistic effect of the employed CO_2-activation of the support and of the selenization procedure applied. A conceivable assumption is that smaller Ru-crystallites (as on Ru/BP$_{act}$) can be stabilized more effectively by Se than larger ones (as on Ru/V).

It was shown [17] that the Se remaining on the catalysts after reductive annealing at 800 °C is exclusively associated with the Ru-nanoparticles and any interaction with the carbon support was abolished. Thus, the optimum Ru:Se ratio should depend on size and shape of the Ru-particles, because only the Ru-surface is modified. For the samples described here, the Ru:Se ratio is ranging from 3:1 for the 5 nm sized particles on the Ru(40 wt.%)Se/V to 5:1 for the 2 nm sized particles on the Ru(40 wt.%)Se/BP$_{act}$ catalyst. It should be noted, that samples with this ratio always show an optimum in electrochemical activity in RDE measurements.

RRDE measurements were performed with varying Se-content of the final conditioned RuSe/BP$_{act}$ catalyst in order to determine the amount of formed H_2O_2. The Se-modification was carried out by impregnation of Ru/BP$_{act}$ with $SeCl_4$ and a subsequent heat treatment at 800 °C in an H_2/N_2 atmosphere. As mentioned above, this procedure leads to complete removal of the inactive excess Se from the carbon support. Therefore, only effects ascribable to the Se-decoration on the Ru-surface are observed. The results are depicted in Fig. 9, and clearly show that the Se-modification leads to a significant decrease in peroxide formation, even at low Se-content. Surprisingly, higher amounts of Se did not lead to a further decrease in H_2O_2

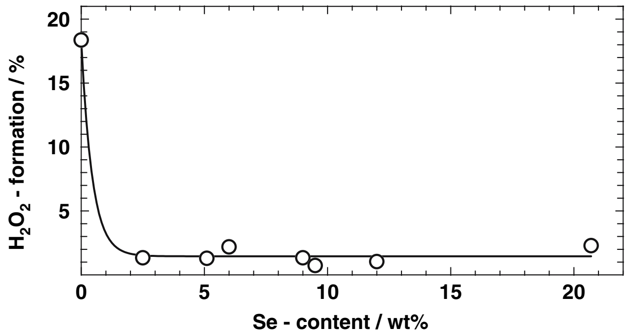

Fig. 9 H_2O_2 yield obtained by RRDE measurements in 0.5 M H_2SO_4 in dependence on the Se content in the used $RuSe_x/BP_{act}$ catalyst

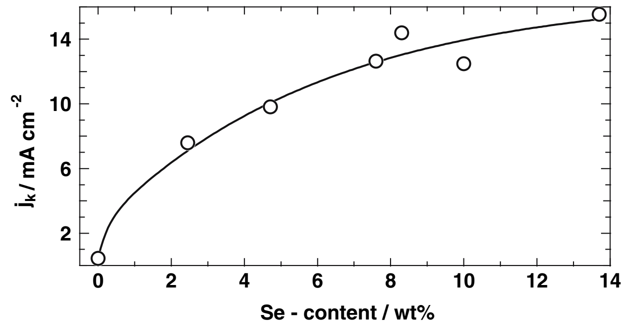

Fig. 10 Kinetic current densities inferred from RDE measurements at U = 0.7 V (NHE) as a function of the Se-content in $RuSe_x$/BP catalysts

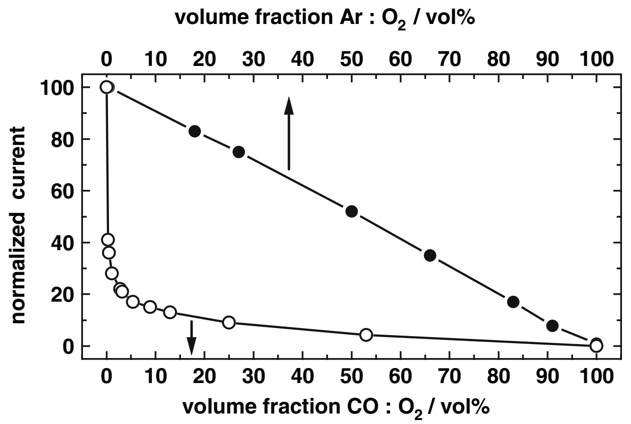

Fig. 11 Normalized current densities in the ORR using a Ru(20 wt.%)Se(1.5 wt.%)/V-XC72 catalyst as electrode in a half cell as a function of volume fraction Ar in O_2 (*upper curve*) and CO in O_2 (*lower curve*)

yield. This trend is in contrast to the obtained dependence of the oxygen reduction current which gradually increases up to a Se-content of about 10 wt.% (Fig. 10). Obviously a small amount of Se is sufficient to inhibit the centers on the Ru-surface which are responsible for H_2O_2-formation, whereas higher amounts of Se form new centers for the direct oxygen reduction to water. Hence Se itself is not known as a good catalyst for oxygen reduction, the interaction of Se and Ru is assumed to be responsible for the high catalytic activity toward the direct reduction mechanism.

The significant change in the electrochemical characteristic of the Ru-particles after treatment with Se also becomes apparent by the electrooxidation of carbon monoxide (CO). Ru-nanoparticles are well known to be a good catalyst for the oxidation of CO to CO_2. This has also been observed on our non-modified Ru/BP material. In CV-measurements performed in the presence of CO-purged electrolyte a distinct anodic current is observed which is attributed to the oxidation of CO. However, with increasing Se-content the CO-oxidation is suppressed. This result clearly shows that the electronic surface structure of the Ru-nanoparticles is significantly changed by modification with Se. In order to get a closer understanding of the suppressed CO-oxidation further measurements were performed in half-cell experiments which enabled us to feed the electrode with well defined mixtures of oxygen and CO or an inert gas like argon. Figure 11 depicts the current densities, which were obtained on a Ru(20 wt.%)Se(1.5 wt.%)/Vulcan catalyst at 0.4 V vs. NHE. Because no CO oxidation is observed on $RuSe_x$-catalysts at this potential the current is only attributed to oxygen reduction. The upper curve depicts the currents observed by varying the volume fraction of Ar in O_2. As expected, the current density decreases linearly with decreasing ratio of oxygen of the loaded gas and points to a reaction order of one with respect to the O_2 concentration. A dramatic change is observed when argon is replaced by CO. The lower curve in Fig. 11 reveals a dramatic decay in oxygen reduction in the presence of <3 vol% CO. Obviously, CO adsorbs onto the $RuSe_x$/C catalyst and inactivates the catalytic centers for oxygen reduction. However, in contrast to metallic non-modified Ru, which also adsorbs CO, the $RuSe_x$-catalyst is unable to oxidize this CO. This effect can tentatively be explained by the occurrence of intermediates in the ORR which are involved in the CO-oxidation mechanism. However, further experiments must be performed in order to clarify this thesis.

4 Conclusion

Electrochemical investigation showed that the surface modification of Ru-nanoparticles with Se leads to more than a tenfold enhancement of the rate of electroreduction of oxygen.

Beside the improvement of the ORR, selenization also enhances stability towards electrochemical oxidation of Ru and its stabilization against migration and aggregation processes.

The key issue for the preparation of highly active catalysts using the described preparation method is the synergism of optimized surface properties of the carbon support affording higher Ru-dispersion and the stabilization of the Ru-particles by modification with Se allowing the removal of excess Se at higher temperatures. Therefore, this method facilitates the preparation of $RuSe_x$-catalysts affording more catalytically active structures on the Ru-surface, compared to conventional materials obtained at lower annealing temperatures on non-activated carbons with adsorption of selenious acid. Investigating the ORR of a Ru(20 wt.%)Se(1.5 wt.%) catalyst at U = 0.4 V vs. NHE as a function of volume fraction CO in O_2 gas an exponential decay of current was monitored in a half cell. The behavior can tentatively be explained either by the blocking of catalytically active sites on the surface of the $RuSe_x$ particles or intermediates in the ORR.

Acknowledgments We thank Dr. D. Alber for the NAA measurements, U. Bloeck for TEM and A. Havemann and I. Rother for assistance in the lab. Financial support from the Federal Ministry of Education and Research and Technology (BMBF) in the frame of the network “O2-RedNet” (contract number 03 SF 0302) is gratefully acknowledged.

References

1. Matthey J (2006) Platinum group metals price bulletin: weekly prices bulletin. Johnson Matthey NY, New York
2. Roskill (2005) Series: Roskill reports on metals & minerals: the economics of platinum group metals. Roskill Information Services, London
3. Wilson MS, Garzon FH, Sickafus KE, Gottesfeld S (1993) J Electrochem Soc 140(10):2872
4. Wang J-T, Wasmus S, Savinell RF (1996) J Electrochem Soc 143(4):1233
5. Neergat M, Shukla AK, Gandhi KS (2001) J Appl Electrochem 31(4):373
6. Dodelet JP (2006) In: Zagal JH, Bedioui F Dodelet JP (eds) N_4-macrocyclic metal complexes. Springer, New York
7. Bogdanoff P, Herrmann I, Hilgendorff M, Dorbandt I, Fiechter S, Tributsch H (2004) J New Mat Electrochem Syst 7(2):85
8. Alonso-Vante N, Bogdanoff P, Tributsch H (2000) J Catal 190(2):240
9. Bron M, Bogdanoff P, Fiechter S, Hilgendorff M, Radnik J, Dorbandt I, Schulenburg H, Tributsch H (2001) J Electroanalyt Chem 517(1–2):85
10. Chatzitheodorou G, *Patent DE 38 02 236 A1* (1988) p 12
11. Alonso-Vante N, *Patent DE 196 44 628 A1* (1996) p 6
12. Hilgendorff M, Diesner K, Schulenburg H, Bogdanoff P, Bron M, Fiechter S (2002) J New Mat Electrochem Syst 5(2):71
13. Bogdanoff P, Fiechter S, Tributsch H, Bron M, Dorbandt I, Hilgendorff M, Schulenburg H, *Patent DE 100 35 841 A1* (2000) p 16
14. Fiechter S, Dorbandt I, Bogdanoff P, Zehl G, Schulenburg H, Tributsch H, Bron M, Radnik J, Fieber-Erdmann M (2007) J Phys Chem C 111(1):477
15. Bron M, Bogdanoff P, Fiechter S, Dorbandt I, Hilgendorf M, Schulenburg H, Tributsch H (2001) J Electroanalyt Chem 500(1–2):510
16. Bönnemann H, Nagabhushana KS (2004) J New Mat Electrochem Syst 7(2):93
17. Zehl G, Dorbandt I, Schmithals G, Radnik J, Wippermann K, Richter B, Bogdanoff P, Fiechter S (2006) ECS Trans 3(1):1261
18. Wippermann K, Richter B, Klafki K, Mergel J, Zehl G, Dorbandt I, Bogdanoff P, Fiechter S, Kaytakoglu S (2006) J Appl Electrochem, doi: 10.1007/s10800-007-9348-7
19. Schulenburg H, Hilgendorf M, Dorbandt I, Radnik J, Bogdanoff P, Fiechter S, Bron M, Tributsch H (2006) J Power Sources 155(1):47